Pionium Lifetime Measurement with DIRAC 2002 and 2003 Ni Data

A. Romero[1,2], B. Adeva[1], J.L. Fungueiriño Pazos[1],
O. Vázquez Doce[1,2],

[1] *IGFAE, University of Santiago de Compostela, Spain*
[2] *INFN, Istituto Nazionale di Fisica Nucleare, Frascati, Italy*

Abstract

After the presentation this year of our final results for Pionium lifetime, using only 2001 Ni data, we now apply the same analysis procedure to the 2002 and 2003 Ni DIRAC data runs. As a result, 10.557 ± 298 atoms are found, which are totally independent, from the statistical point of view, from those found in the 2001 data. A specific Monte Carlo simulation has been carried out for the new data. The main differences in the spectrometer with respect to 2001, which have deserved new simulations, are the presence of a new detector upstream, the SFD U-plane, and the lower proton beam momentum of 20 GeV/c. Results are presented for the combined 2002+2003 sample, in order to show the peculiarities and relative quality of this analysis with respect to 2001. A separate note is issued for an integrated analysis of the full DIRAC pNi data, including final lifetime results, with a single representation of the spectra.

DIRAC internal note 07-15 *2 November 2007*

1 Analysis method and corrections

1.1 Statistical analysis method

For the sake of completeness we remind here the definition [1] of the χ^2 in the analysis of the prompt $2D$ spectrum in (Q_T, Q_L) plane :

$$\chi^2 = \sum_j \frac{\left(N_p^j - \beta(\alpha_1[\epsilon\frac{N_{KK}^j}{N_{KK}} + (1-\epsilon)\frac{N_{CC}^j}{N_{CC}}] - \alpha_2\frac{N_{AC}^j}{N_{AC}} - \alpha_3\frac{N_{NC}^j}{N_{NC}} - \gamma\frac{N_{AA}^j}{N_{AA}})\right)^2}{N_p^j + \beta^2(\alpha_1^2[(1-\epsilon)^2\frac{N_{CC}^j}{N_{CC}^2} + \epsilon^2\frac{N_{KK}^j}{N_{KK}^2}] + \alpha_2^2\frac{N_{AC}^j}{N_{AC}^2} + \alpha_3^2\frac{N_{NC}^j}{N_{NC}^2} + \gamma^2\frac{N_{AA}^j}{N_{AA}^2})} \quad (1)$$

where α_i and γ are the respective Monte Carlo type fractions (constraint by $\alpha_1 + \alpha_2 + \alpha_3 + \gamma = 1$), β represents the global normalization of the Monte Carlo, which corresponds essentially to the total number of prompt events in the fit region [1] . N_p^j, N_{CC}^j, N_{AC}^j, N_{NC}^j, N_{AA}^j are the number of prompt, Coulomb, accidental, non-Coulomb and atom pairs, respectively, in each $2D$ bin, as described in our previous note [1]. Correspondingly, N_p, N_{CC}, N_{AC}, N_{NC}, N_{AA} are the total number of events in the fit region.

A **control region** is defined by the domain under the cut $Q_L > 2MeV/c$. We call $Q_L < 2MeV/c$ the **extrapolation region**. Errors are obtained by χ^2 variation of one unit. The fit strategy is to perform a preliminary fit that includes the Pionium Monte Carlo in the linear combination. Then the latter is subtracted and the difference between the prompt and the Monte Carlo spectrum is analysed in detail, in order to measure the number of atom pairs. The breakup probability is then determined by means of the K-factors [1].

The χ^2-fit is performed either globally, including all statistics, as reported in section 2, or at ten individual pair momentum $600MeV/c$ bins, as will be seen in section 3.

[1] more detailed definitions will be provided in subsection 2.2

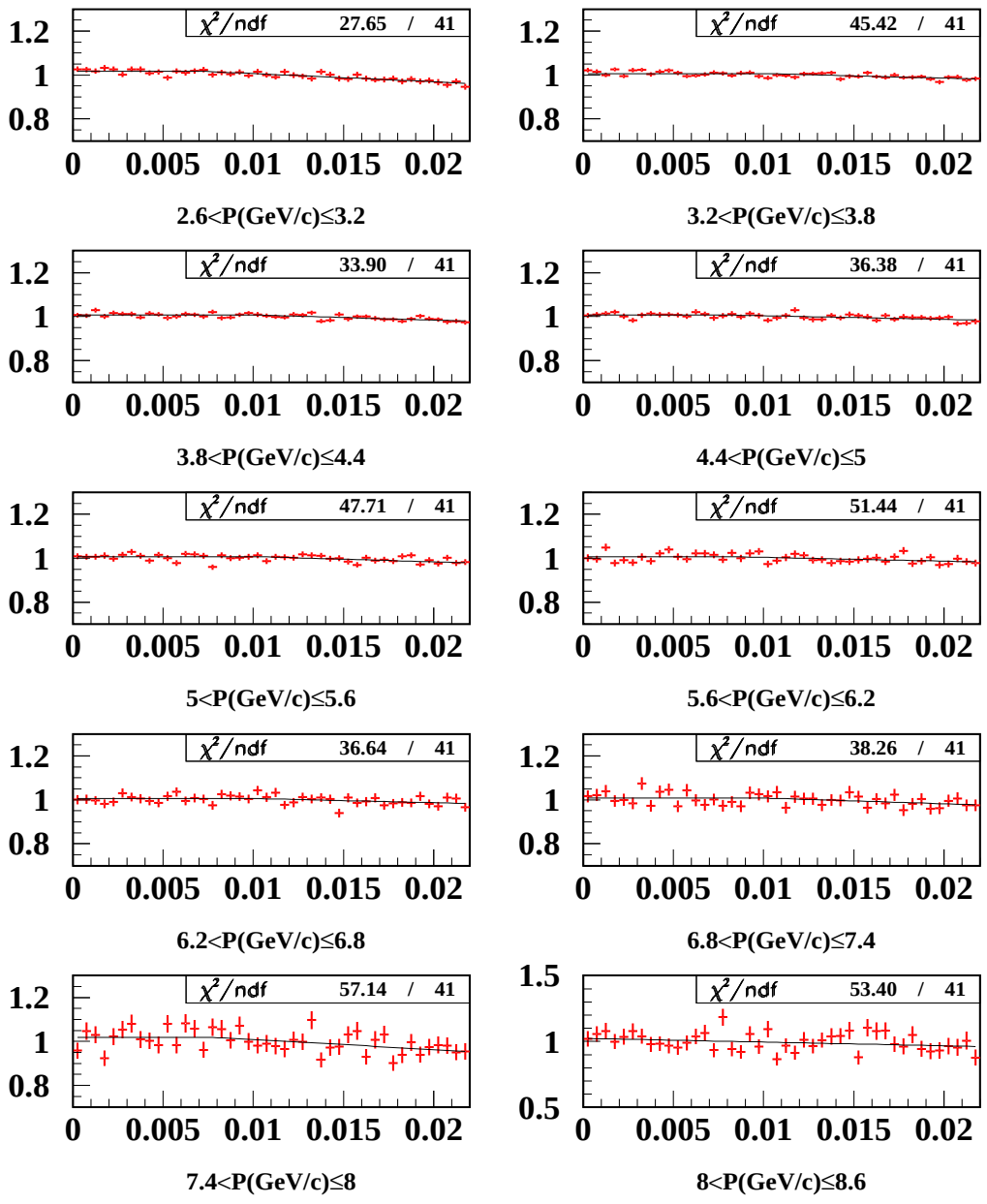

Fig. 1. *Q_L spectrum of the ratio between accidental pairs from the spectrometer and non-Coulomb Monte Carlo, in ten 600 MeV/c bins of lab-frame pair momentum p. The line shows a parametric fit to the data, which was used as a correction for the prompt pairs. Fit χ^2-values are indicated.*

1.2 Accidental pairs

The fraction of accidental pairs inside the prompt coincidence has been experimentally determined, from analysis of the precision TOF spectrum. It was determined as function of the pair momentum, and separately for 2002 and 2003 data, and the results are given in table 1 and figure 2. For the sake of reference, also the 2001 data are given.

The Vertical Hodoscope resolution remained approximately constant for the experiment's lifetime, however amount of background increased in 2002 and 2003, probably due to the effect of increased average beam intensity.

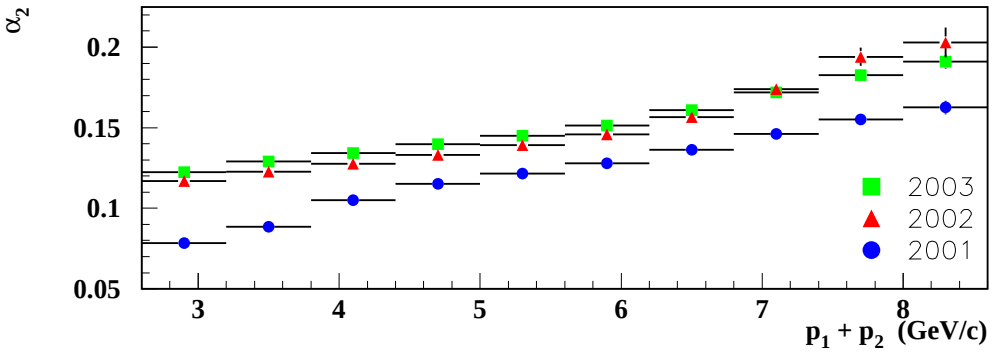

Fig. 2. *Accidental pair fractions in table 1 as function of pair momentum.*

Table 1
Accidental pair contamination inside the prompt coincidence, as determined from analysis of the TOF spectrum. Data are given for each datataking year.

	p (GeV/c)	% 2001	% 2002	% 2003
p_1	2.6 - 3.2	0.0783 ± 0.0007	0.1225 ± 0.0006	0.1169 ± 0.0011
p_2	3.2 - 3.8	0.0886 ± 0.0007	0.1289 ± 0.0007	0.1228 ± 0.0013
p_3	3.8 - 4.4	0.1051 ± 0.0007	0.1343 ± 0.0006	0.1276 ± 0.0010
p_4	4.4 - 5.0	0.1152 ± 0.0008	0.1397 ± 0.0006	0.1332 ± 0.0012
p_5	5.0 - 5.6	0.1216 ± 0.0009	0.1451 ± 0.0008	0.1391 ± 0.0015
p_6	5.6 - 6.2	0.1281 ± 0.0010	0.1513 ± 0.0009	0.1460 ± 0.0018
p_7	6.2 - 6.8	0.1362 ± 0.0014	0.1609 ± 0.0013	0.1565 ± 0.0024
p_8	6.8 - 7.4	0.1462 ± 0.0019	0.1720 ± 0.0018	0.1738 ± 0.0036
p_9	7.4 - 8.0	0.15525 ± 0.0027	0.1826 ± 0.0026	0.1940 ± 0.0057
p_{10}	8.0 - 8.6	0.1625 ± 0.0041	0.1909 ± 0.0042	0.2030 ± 0.0093

1.3 Summary of corrections

Several small corrections to the data have been reported in our previous work [1], [2], which description we are not repeating here. Let us simply recall the status of these corrections in the present analysis:

- A Q_L trigger acceptance correction is done based upon the behaviour of accidental pairs, shown in Fig. 1. Good quality χ^2-fits to our parametrization (despite the increased statistics in accidental pairs with respect to 2001 data), will reveal genuine agreement between prompt pairs and standard Coulomb interaction, when this correction is applied in sections 2 and 3.
- K^+K^- contamination correction is done using Monte Carlo and real data, as explained in [1].
- the small Q_T correction reported in [2] is no longer needed here (it is zero), due to complete agreement between data and Monte Carlo in the control region. This is a consequence of the improved quality of the data in the upstream arm (MSGC/GEM and SFD).
- the target impurity correction is done according to reference [5], as before [1]
- no finite-size correction appears to be necessary, as in [1]. The significance for this has increased considerably, as it will be seen below in tables 4, 11 and 12.

2 Global fit analysis

2.1 K-factors calculation

For completeness, we provide in table 2 the K-factors for the p-integrated case (global fit) and in table 3 the p-dependent ones, for the standard cuts $Q_T < 5MeV/c$ and $Q_L < 2MeV/c$. Both are entirely consistent with those calculated for 2001 data.

2.2 Global fit results

The global fit consists in minimizing the χ^2 defined in (1) in $2D$ with respect to α_3 (non-Coulomb fraction) and γ parameters, using the momentum-integrated sample. The α_2 and ϵ parameters remain fixed in this fit, and α_2 is determined by the direct measurement of the accidental pairs fraction from the analysis

Table 2
Numerical values of K^{th} and K^{exp} as defined in reference [2], obtained for our improved Monte Carlo simulation. Each raw corresponds to a given rectangular cut in (Q_T, Q_L) plane , with $Q_T^c = 5MeV/c$ and $Q_L^c = 2MeV/c$ being the reference cut values. No practical change is observed with respect to earlier values.

$Q_L^{cut}(MeV/c)$	K^{theo}	K^{exp}
0.5	0.4372	0.2937 ± 0.0009
1.0	0.2389	0.2135 ± 0.0005
1.5	0.1669	0.1581 ± 0.0003
2.0	0.1300	0.1246 ± 0.0002
$Q_T^{cut}(MeV/c)$	K^{theo}	K^{exp}
0.5	3.2457	0.9319 ± 0.0089
1.0	1.2382	0.6963 ± 0.0037
1.5	0.6995	0.5224 ± 0.0020
2.0	0.4674	0.3965 ± 0.0012
2.5	0.3426	0.3089 ± 0.0008
3.0	0.2660	0.2465 ± 0.0006
3.5	0.2147	0.2017 ± 0.0004
4.0	0.1781	0.1687 ± 0.0004
4.5	0.1509	0.1438 ± 0.0003
5.0	0.1300	0.1246 ± 0.0002

of the precision time-of-flight spectrum. ϵ is fixed to the K^+K^- fraction experimentally determined and used in [1]. β can either be left as a free parameter, or be fixed to the total number of prompt pairs in the fir region (N_p), or to the ratio $\beta = N_p^c/f_c$ where N_p^c is the number of prompt events with $Q_L > 2MeV/c$ (control region) and f_c is the ratio between the number of Monte Carlo pairs in the control region and the total number of Monte Carlo events. These choices are small variations with respecto to N_p and produce slight changes in the fit results, as indicated in table 6.

We have chosen to perform the fit in 0.25×0.25 $(MeV/c)^2$ bins in the (Q_T, Q_L) plane, for the global fit. Variations with respect to this choice will be reported in table 6.

Once the fit has converged, we define the atom signal in each (i, j) bin as the difference between the prompt spectrum (with accidentals subtracted as explained before) and the Monte Carlo with the Pionium component (AA) removed. This 2D signal, which reveals the excess with respect to the calculated

Coulomb interaction enhancement background, is what we call the Pionium spectrum. The atom breakup probability P_{br} is then determined [2] by means of the K-factors.

Just as we did with the 2001 data [1], we present the fit results in several steps. The correction sequence is defined in a cumulative way, namely:

a) use improved statistics Monte Carlo.
b) include K^+K^- correction.
c) perform the target impurity correction.
d) remove the finite-size correction.

In table 4 we present the χ^2 values (separately in control and extrapolation regions), the number of atoms N_A, the number of Coulomb pairs in the complete fit range N_{CC}, the β parameter and the P_{br} for each option.

Please note that whereas the introduction of the K^+K^- contamination decreases the total χ^2 by 5.1 units, the removal of the finite-size correction decreases it by 12.7 units. The combined effect of both actions decreased the total χ^2 by 17.8 units. We remark that, in agreement with our earlier findings, the finite-size correction is not wanted by the data. The statistical significance will be further enhanced when we report the momentum-dependent fit in subsection 3.1.

Table 3
K-factors determined in 10 intervals of laboratory-frame momentum, re-evaluated for the new Monte Carlo simulation.

p interval (GeV/c)	$K-factor$
2.6-3.2	0.1105 ± 0.0005
3.2-3.8	0.1173 ± 0.0004
3.8-4.4	0.1237 ± 0.0005
4.4-5.0	0.1294 ± 0.0006
5.-5.6	0.1334 ± 0.0007
5.6-6.2	0.1373 ± 0.0008
6.2-6.8	0.1396 ± 0.0011
6.8-7.4	0.1457 ± 0.0015
7.4-8.0	0.1459 ± 0.0022
8.-8.6	0.1453 ± 0.0032

Table 4
Fit results for the correction options $a), b), c), d))$ indicated in the text. χ^2's in the full domain, and its restriction to the control and extrapolation regions separately, are given. Also the total number of atoms N_A and coulomb pairs N_{CC}, the β parameter and the break-up probabilities are indicated.

	a)	a+b)	a)+b)+c)	a)+b)+c)+d)
χ^2_{tot}/ndf	1675.4/1600	1670.3/1600	1670.3/1600	1657.6/1600.0
χ^2_{ext}/ndf	171.5/160	168.0/160	168.0/160	167.1/160
χ^2_{cont}/ndf	1503.9/1440	1502.3/1440	1502.3/1440	1490.5/1440
N_A	10826 ± 307	10406 ± 295	10406 ± 295	10557 ± 298
N_{CC}	1290416 ± 7305	1270596 ± 7177	1270596 ± 7177	1255217 ± 7111
β	1601905	1601931	1601930	1601954
P_{Br}	0.421 ± 0.013	0.411 ± 0.013	0.417 ± 0.013	0.427 ± 0.013

In addition, we illustrate here again an effect that was already pointed out with 2001 data [1], namely that the K^+K^- correction introduces a significantly better stability of the measured P_{Br} values with respect to the Q_T cut, and also a better agreement between the Q_T and Q_L series of cuts to define the atom signal, at the limit of very low Q_T and Q_L values, as it can be clearly appreciated in the figure 11.

As far as the K^+K^- correction is concerned, we have made the exercise of letting the ϵ parameter free in the fit. When this is done, we obtain $\epsilon = 0.0138$ $\pm$ 0.0053 which is entirely compatible with the value $\epsilon = 0.0072$ used in the fit, determined from our measurement [3].

The Pionium $2D$ signal is shown in the form of lego plots in figures 9 and 10.

Table 5
Comparison of global fit results for three different choices of the β parameter definition.

	β	P_{Br}	χ^2/ndf
β all range	1603179	0.419 ± 0.013	1658.3/1600
β ($Q_L > 2MeV/c$)	1602820	0.424 ± 0.013	1658.0/1600
β free	1601954	0.427 ± 0.013	1657.6/1600

Table 6
Comparison of global fit results using two different (Q_T, Q_L) binsizes.

	β	P_{Br}	χ^2/ndf
0.25×0.25	1601954	0.427 ± 0.013	1657.6/1600
0.5×0.5	1602913	0.426 ± 0.013	358.7/400

2.3 Dependence on the Q_L upper limit

Our standard fit domain is the region $Q_L < 20MeV/c$ and $Q_T < 5MeV/c$, and the dependence of the P_{Br} with respect to the Q_L upper limit (Q_L^{up}) is analysed in table 7. We see how the P_{Br} fluctuates in a random way, with no appreciable systematics, and that the value at $Q_L^{up} = 20MeV/c$ is close to the average.

Table 7
Values of break-up probability P_{Br} obtained from different choices of the upper limit (Q_L^{cut}) used to define the control region in Q_L projection.

$Q_L^{cut}(MeV/c)$	P_{Br}
22	0.424 ± 0.013
21	0.428 ± 0.013
20	0.427 ± 0.013
19	0.424 ± 0.013
18	0.418 ± 0.013
17	0.420 ± 0.013
16	0.420 ± 0.014
15	0.422 ± 0.014
14	0.425 ± 0.014
13	0.419 ± 0.014

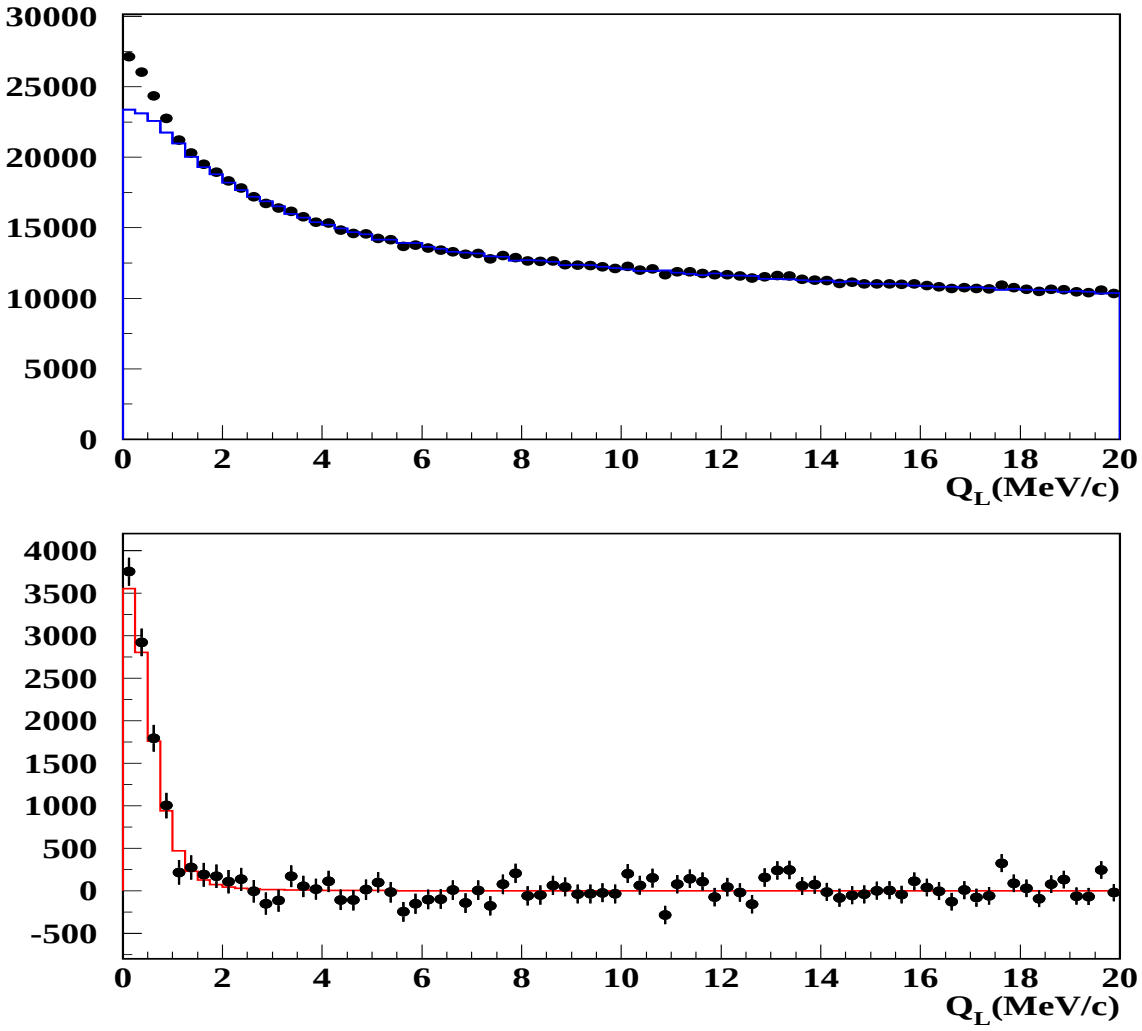

Fig. 3. *Two-dimensional global fit projection onto Q_L. The standard $Q_T < 4$ MeV/c cut has been applied. The difference between prompt data (dots) and Monte Carlo (blue line), which corresponds to Pionium signal, is plotted at the bottom, where the signal is compared with the Pionium atom Monte Carlo (red line).*

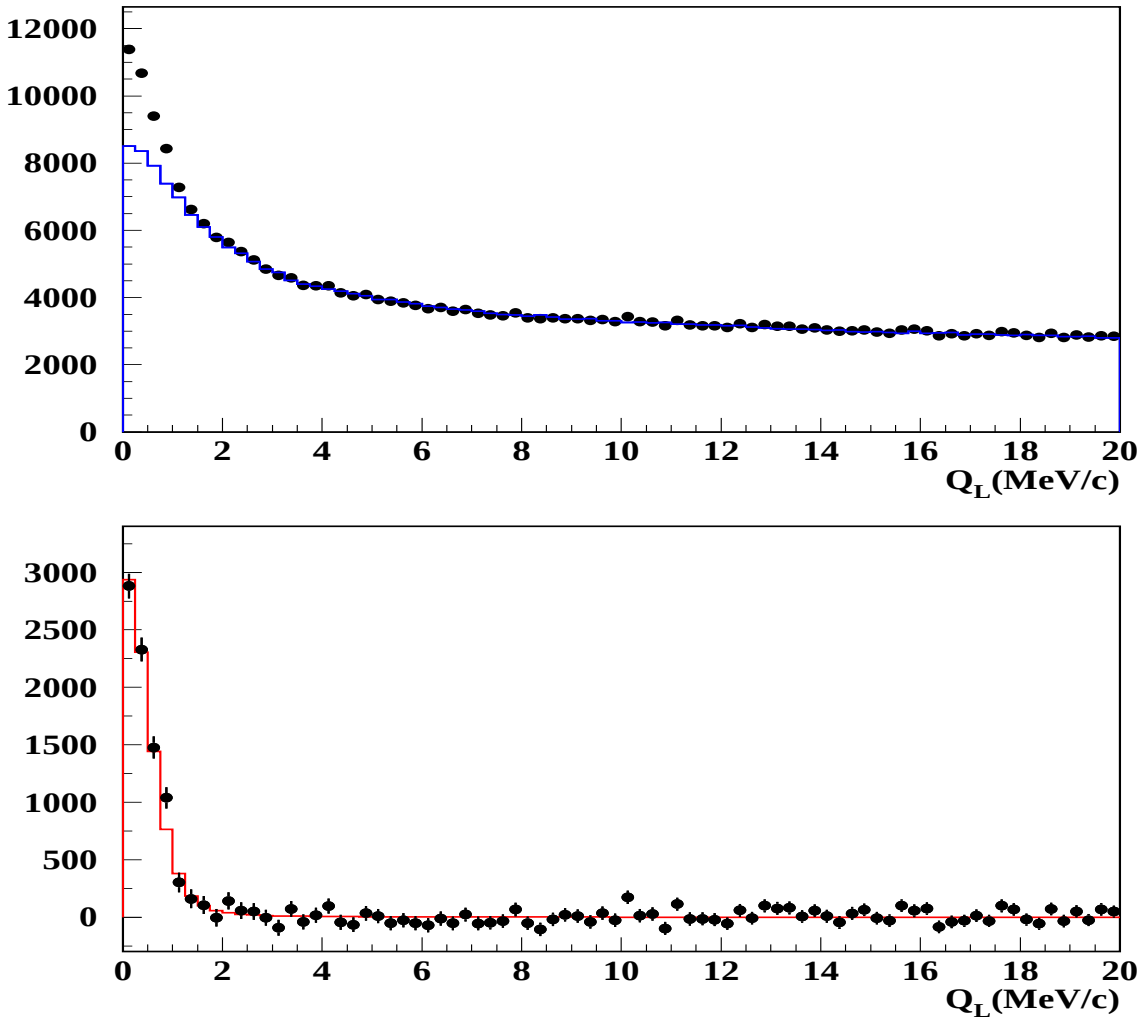

Fig. 4. *Two-dimensional global fit projection onto Q_L. A more restrictive $Q_T < 2$ MeV/c cut has been applied to enhance the signal. The difference between prompt data (dots) and Monte Carlo (blue line), which corresponds to Pionium signal, is plotted at the bottom, where the signal is compared with the Pionium atom Monte Carlo (red line).*

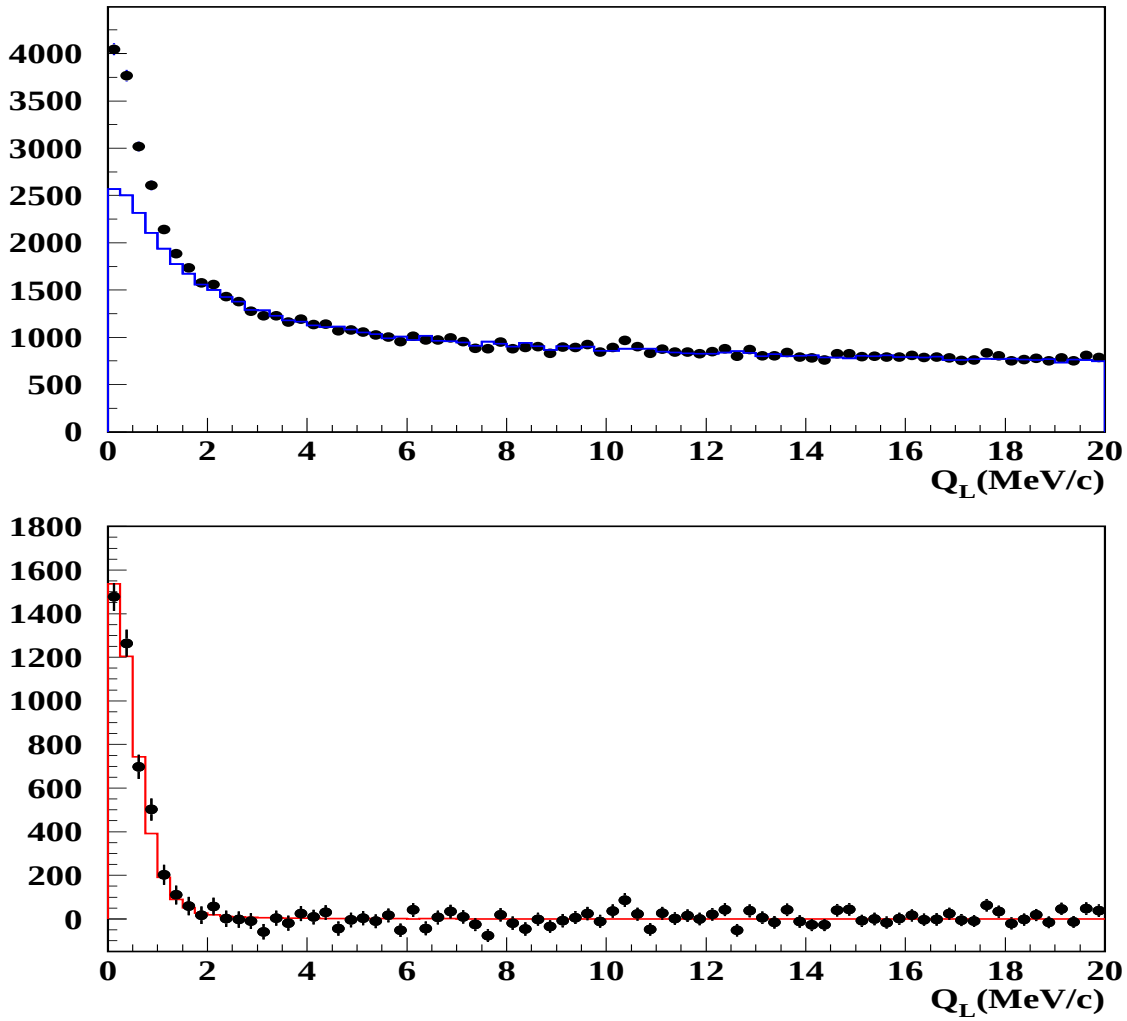

Fig. 5. *Two-dimensional global fit projection onto Q_L. A more restrictive $Q_T < 1$ MeV/c cut has been applied to enhance the signal. The difference between prompt data (dots) and Monte Carlo (blue line), which corresponds to Pionium signal, is plotted at the bottom, where the signal is compared with the Pionium atom Monte Carlo (red line).*

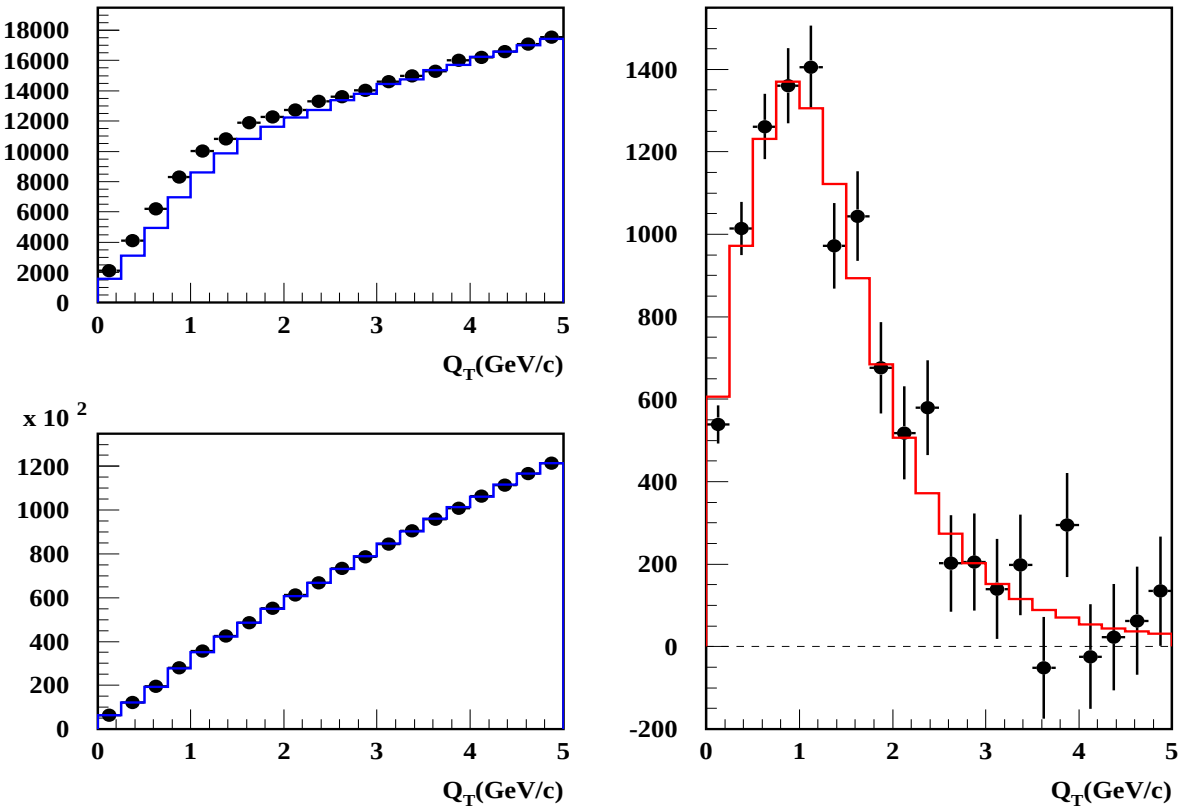

Fig. 6. *Two-dimensional global fit projection onto Q_T. The data are shown separately for $Q_L < 2MeV/c$ (left top) and $Q_L > 2MeV/c$ (left bottom). The difference between prompt data (dots) and Monte Carlo (blue line), which corresponds to transverse Pionium signal, is plotted (right) and compared with the Pionium atom Monte Carlo (red line).*

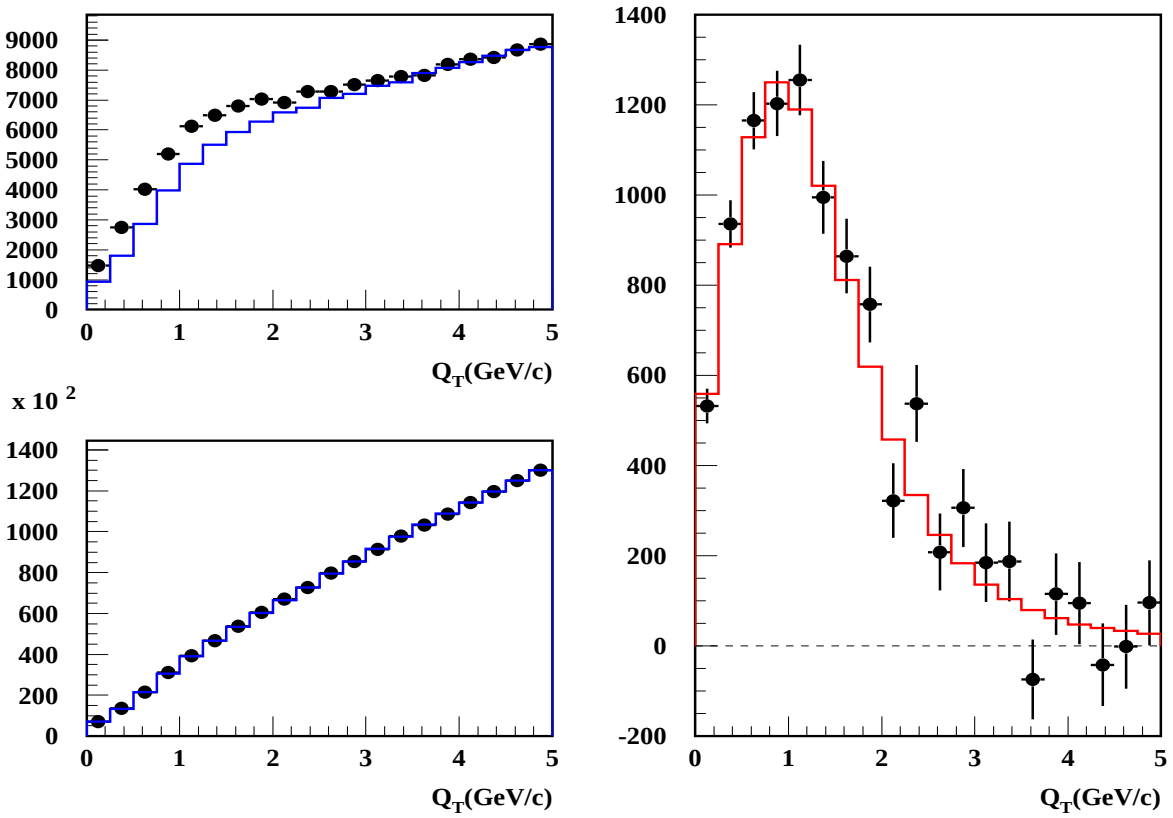

Fig. 7. *Two-dimensional global fit projection onto Q_T. The data are shown separately for $Q_L < 1MeV/c$ (left top) and $Q_L > 1MeV/c$ (left bottom). The difference between prompt data (dots) and Monte Carlo (blue line), which corresponds to transverse Pionium signal, is plotted (right) and compared with the Pionium atom Monte Carlo (red line).*

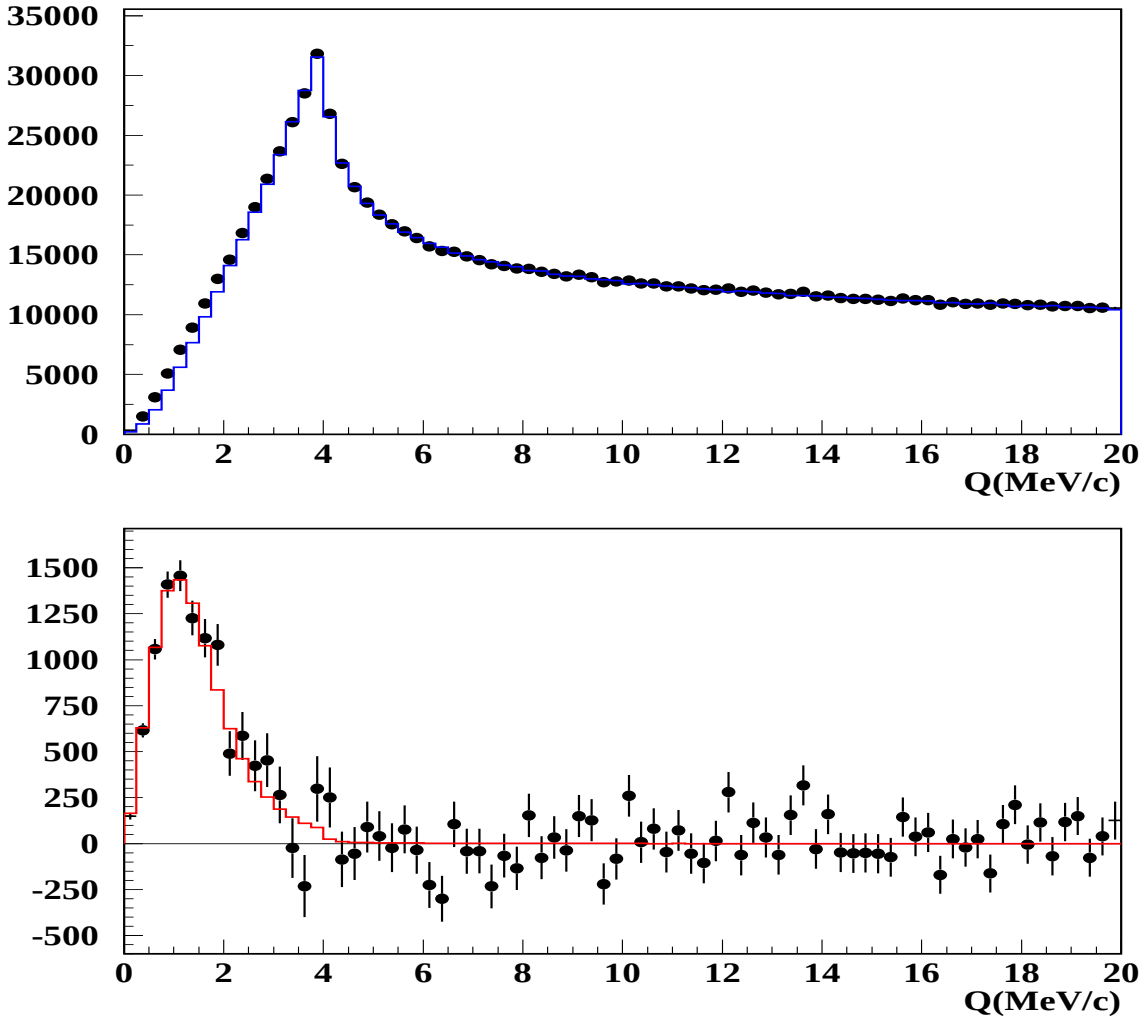

Fig. 8. *Two-dimensional global fit projection onto Q. The standard $Q_T < 4MeV/c$ cut was applied. The difference between prompt data (dots) and Monte Carlo (blue line), which corresponds to Pionium signal, is plotted at the bottom. The signal is compared with the Pionium atom Monte Carlo (red line).*

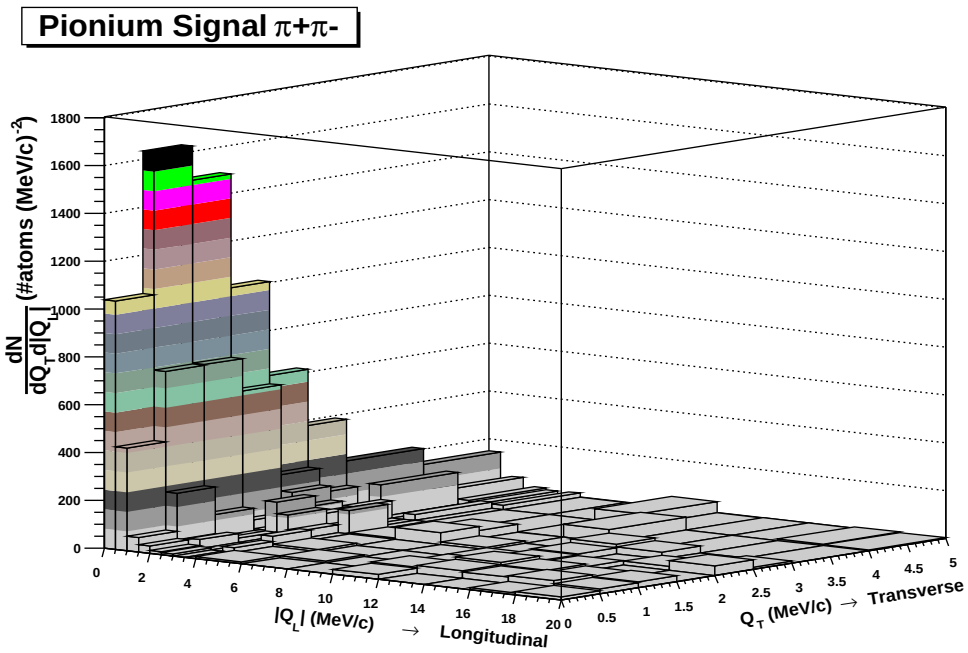

Fig. 9. *Lego plot showing the Pionium break-up spectrum in Ni in the* $(Q_T, Q_L = |Q_Z|)$ *plane, after subtraction of the Coulomb background.*

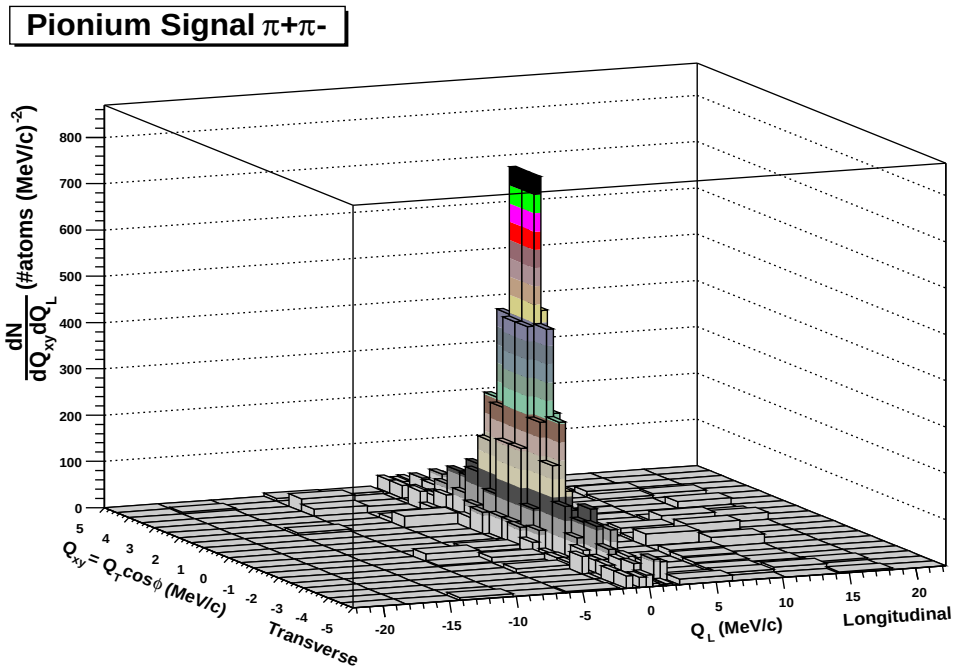

Fig. 10. *Lego plot showing the Pionium break-up spectrum in Ni in the* (Q_{xy}, Q_L) *plane, after subtraction of Coulomb background. The transverse component* $Q_{xy} = Q_T\ cos\phi$ *is defined as the product of the measured* Q_T *value times the cosine of a random azimuth.*

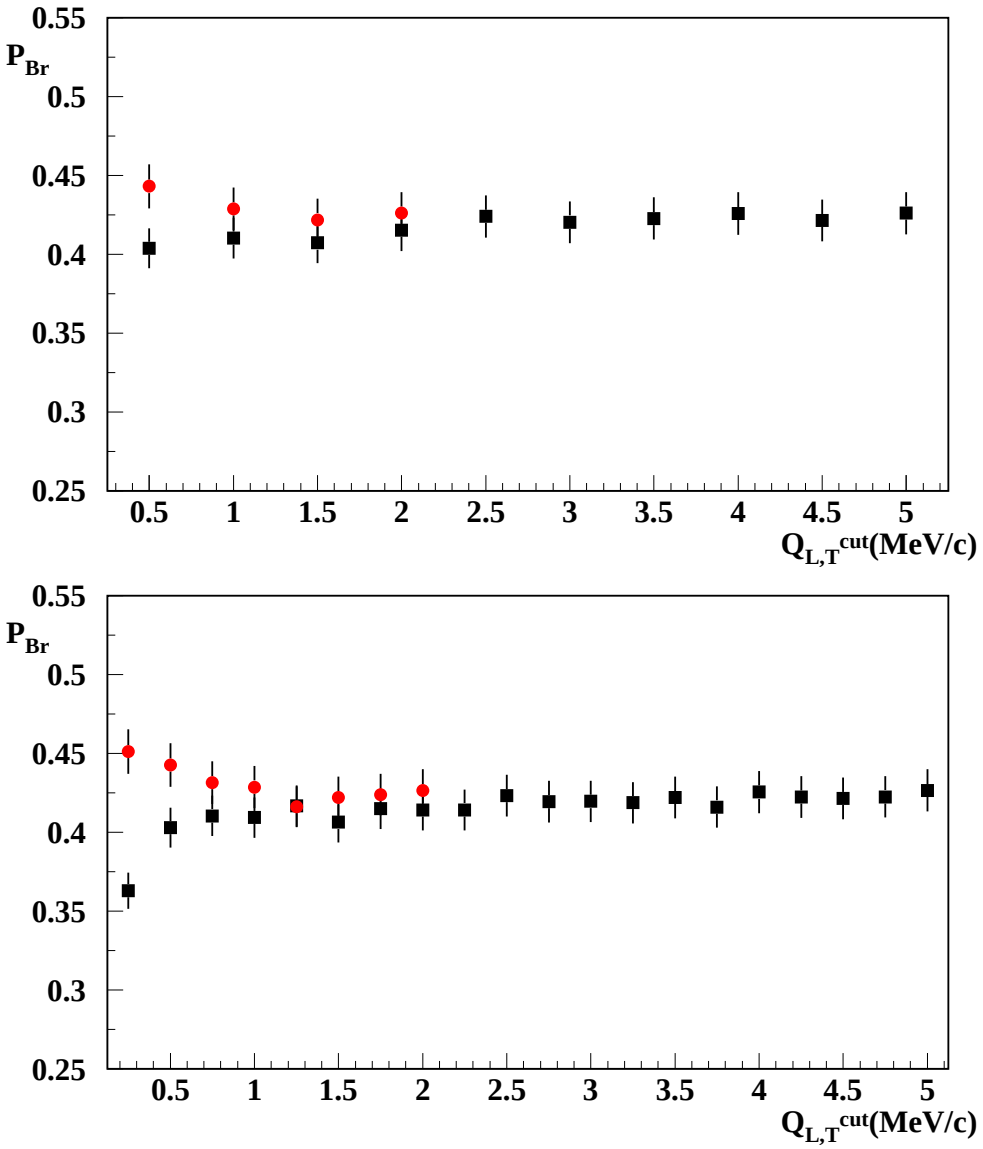

Fig. 11. *Pionium break-up probabilities determined from different choices of the upper limits ($Q^u_{T,L}$) in the rectangular integration domain to define the atom signal. Top plot shows the 2002+2003 results after the introduction of K^+K^- correction, in $0.5 MeV/c$ steps of Q^u_L (red dots) and Q^u_T (black squares). Bottom plot shows the same in $0.25 MeV/c$ steps.*

3 Momentum-dependent analysis

Following the approach of our earlier work [2], in this section we split the pair momentum spectrum in ten 600 MeV/c bins and perform independent fits at each momentum interval. The corrections applied are the same as for the global fit. The only change with respect to the latter is the choice of $0.5 \times 0.5(MeV/c)^2$ binsize, which is now obliged due to the strong statistics reduction at individual 2D bins. We use the same definition of β as in section 2.2.

3.1 Fit results

As we did with 2001 data, we now present the final results after the introduction of all corrections, in order to avoid proliferation of figures. However, we keep record of the individual changes at each step, by giving the p-dependent and global fit results in the form of tables, distributed as follows:

a) Table 9: The new Monte Carlo is used.
b) Table 10: K^+K^- contamination is introduced, after the parametrization given in [1].
c) Table 11: New Monte Carlo, K^+K^- contamination and target impurity correction.
d) Table 12: In addition to the above, the finite-size correction is dropped.

Figures from 12 to 21 show the result of the 10 independent fits in the form of atom spectra (Q_L and Q_T) and break-up probabilities as function of Q_L and Q_T cuts.

The Pionium line-shape shows good agreement between the prompt data signal and the Monte Carlo.

In table 8 a new global χ^2 has been defined as the sum of the individual ones at each momentum bin, and a combined P_{Br} value and error have been calculated after proper account of the independent statistical errors. The number of atoms (N_A) and Coulomb pairs (N_C) are also indicated.

From table 8 we draw the same conclusions as from the global analysis. The introduccion of K^+K^- simulation improves the χ^2 by 10.7 units, and when the finite-size correction is removed, the χ^2 improves by 32.5 additional units. We consider this a clear indication that the latter should be done. Adding this two changes, the χ^2 is reduced by 46.2 units.

Table 8
Combined momentum dependent fit, for progressive fit conditions as defined in the text.

	A	A+B	A+B+C	A+B+C+D
χ^2	3207.5/3157	3200.1/3157	3200.1/3157	3175.2/3157
P_{Br}	0.418 ± 0.014	0.414 ± 0.014	0.420 ± 0.014	0.427 ± 0.014
N_A	10741 ± 320	10465 ± 313	10465 ± 313	10553 ± 315
N_C	869436 ± 5515	857043 ± 5427	857043 ± 5427	847754 ± 5383

Table 9
Results of the momentum-dependent fit, using correction a) only (see text). Break-up probability values P_{Br}, number of atom pairs N_A, α_1 and χ^2 over the entire fit region are indicated in this table, for every 600 MeV/c momentum interval p_i as defined in table 3.

	P_{Br}	N_A	α_1	χ^2 /ndf	χ^2_e / ndf
p_1	0.375 ± 0.035	1289 ± 107	0.788 ± 0.013	301.4 / 288	27.3 / 32
p_2	0.467 ± 0.031	2533 ± 149	0.791 ± 0.010	289.9 / 288	33.1 / 32
p_3	0.377 ± 0.028	1887 ± 127	0.822 ± 0.011	274.2 / 288	26.0 / 32
p_4	0.407 ± 0.032	1596 ± 112	0.812 ± 0.013	282.8 / 288	21.5 / 32
p_5	0.425 ± 0.044	1291 ± 120	0.842 ± 0.015	267.7 / 288	25.9 / 32
p_6	0.462 ± 0.049	945 ± 87	0.807 ± 0.019	341.8 / 288	29.6 / 32
p_7	0.486 ± 0.073	598 ± 78	0.811 ± 0.025	316.0 / 288	44.5 / 32
p_8	0.525 ± 0.161	354 ± 98	0.804 ± 0.036	312.6 / 288	45.3 / 32
p_9	0.495 ± 0.143	160 ± 41	0.764 ± 0.046	284.9 / 282	23.4 / 32
p_{10}	0.787 ± 0.247	89 ± 21	0.612 ± 0.070	234.9 / 251	24.7 / 32

Table 10
Results of the momentum-dependent fit, using corrections a+b (see text). Break-up probability values P_{Br}, number of atom pairs N_A, α_1 and χ^2 over the entire fit region are indicated in this table, for every 600 MeV/c momentum interval p_i as defined in table 3.

	P_{Br}	N_A	α_1	χ^2 /ndf	χ^2_e / ndf
p_1	0.373 ± 0.035	1275 ± 106	0.786 ± 0.013	301.9 / 288	27.2 / 32
p_2	0.465 ± 0.031	2504 ± 148	0.788 ± 0.010	289.4 / 288	33.4 / 32
p_3	0.373 ± 0.028	1847 ± 125	0.817 ± 0.011	274.3 / 288	26.5 / 32
p_4	0.401 ± 0.032	1548 ± 110	0.806 ± 0.013	282.7 / 288	21.9 / 32
p_5	0.416 ± 0.044	1239 ± 117	0.835 ± 0.015	266.0 / 288	25.1 / 32
p_6	0.452 ± 0.049	902 ± 84	0.797 ± 0.019	341.2 / 288	28.7 / 32
p_7	0.482 ± 0.073	575 ± 76	0.798 ± 0.024	315.6 / 288	43.1 / 32
p_8	0.519 ± 0.160	337 ± 94	0.790 ± 0.035	312.2 / 288	43.8 / 32
p_9	0.481 ± 0.140	150 ± 38	0.750 ± 0.046	285.1 / 282	22.4 / 32
p_{10}	0.816 ± 0.257	87 ± 21	0.595 ± 0.068	235.3 / 251	24.5 / 32

Table 11
Fit results of the momentum-dependent fit, using corrections a+b+c (see text). Break-up probability values P_{Br}, number of atom pairs N_A, α_1 and χ^2 over the entire fit region are indicated in this table, for every 600 MeV/c momentum interval p_i as defined in table 3.

	P_{Br}	N_A	α_1	χ^2 /ndf	χ^2_e / ndf
p_1	0.378 ± 0.035	1275 ± 106	0.786 ± 0.013	301.9 / 288	27.2 / 32
p_2	0.472 ± 0.031	2504 ± 148	0.788 ± 0.010	289.4 / 288	33.4 / 32
p_3	0.378 ± 0.029	1847 ± 125	0.817 ± 0.011	274.3 / 288	26.5 / 32
p_4	0.406 ± 0.032	1548 ± 110	0.806 ± 0.013	282.7 / 288	21.9 / 32
p_5	0.422 ± 0.044	1239 ± 117	0.835 ± 0.015	266.0 / 288	25.1 / 32
p_6	0.458 ± 0.049	902 ± 84	0.797 ± 0.019	341.2 / 288	28.7 / 32
p_7	0.489 ± 0.074	575 ± 76	0.798 ± 0.024	315.6 / 288	43.1 / 32
p_8	0.526 ± 0.162	337 ± 94	0.790 ± 0.035	312.2 / 288	43.8 / 32
p_9	0.488 ± 0.142	150 ± 38	0.750 ± 0.046	285.1 / 282	22.4 / 32
p_{10}	0.827 ± 0.261	87 ± 21	0.595 ± 0.068	235.3 / 251	24.5 / 32

Table 12
Final fit results of the momentum-dependent fit, using all corrections a+b+c+d (see text). Break-up probability values P_{Br}, number of atom pairs N_A, α_1 and χ^2 over the entire fit region are indicated in this table, for every 600 MeV/c momentum interval p_i as defined in table 3.

	P_{Br}	N_A	α_1	χ^2 /ndf	χ^2_e / ndf
p_1	0.386 ± 0.036	1291 ± 107	0.777 ± 0.013	299.7 / 288	27.1 / 32
p_2	0.481 ± 0.032	2534 ± 149	0.779 ± 0.010	286.5 / 288	33.2 / 32
p_3	0.386 ± 0.029	1873 ± 126	0.807 ± 0.011	272.2 / 288	26.0 / 32
p_4	0.413 ± 0.033	1564 ± 110	0.797 ± 0.013	280.7 / 288	21.8 / 32
p_5	0.429 ± 0.045	1250 ± 117	0.826 ± 0.015	264.0 / 288	25.0 / 32
p_6	0.463 ± 0.050	906 ± 85	0.789 ± 0.018	338.1 / 288	28.6 / 32
p_7	0.492 ± 0.074	576 ± 76	0.790 ± 0.024	313.6 / 288	42.7 / 32
p_8	0.520 ± 0.162	332 ± 94	0.784 ± 0.035	309.4 / 288	43.1 / 32
p_9	0.469 ± 0.139	144 ± 37	0.748 ± 0.045	282.9 / 282	22.3 / 32
p_{10}	0.778 ± 0.248	83 ± 20	0.599 ± 0.068	233.9 / 251	24.5 / 32

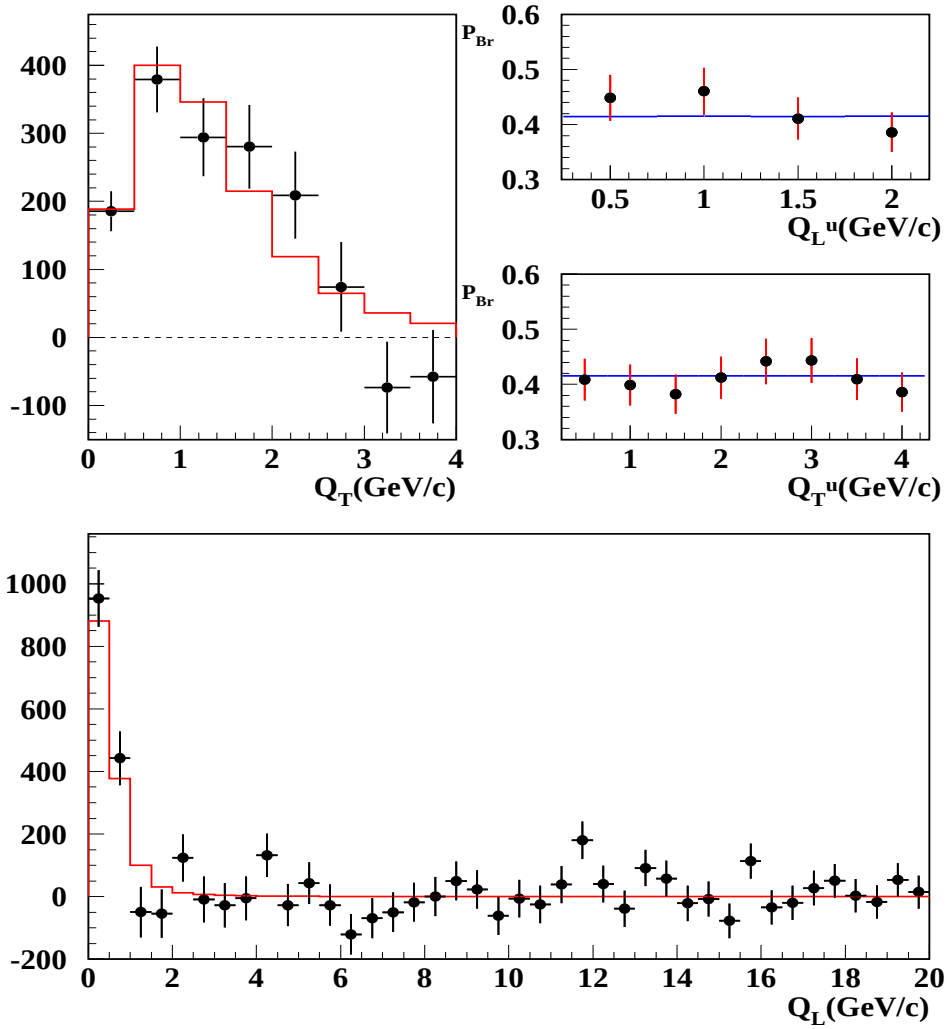

Fig. 12. *Fit results for the $\pi^+\pi^-$ momentum bin $2.6 < p < 3.2$ GeV/c in lab-frame. Q_T (top left) and Q_L (botom) projections of the atom signal found in the extrapolation region ($Q_L < 2MeV/c$) after subtraction of the Monte Carlo prediction with Pionium component removed. Values of break-up probability determined for different integration upper limits Q_T^u and Q_L^u to define the atom signal (top right). Note the different Q_L^u values are all defined for $Q_T^u = 5MeV/c$ and Q_T^u values are defined for $Q_L^u = 2MeV/c$. The blue line indicates the P_{Br} determined from atom counting using the Monte Carlo.*

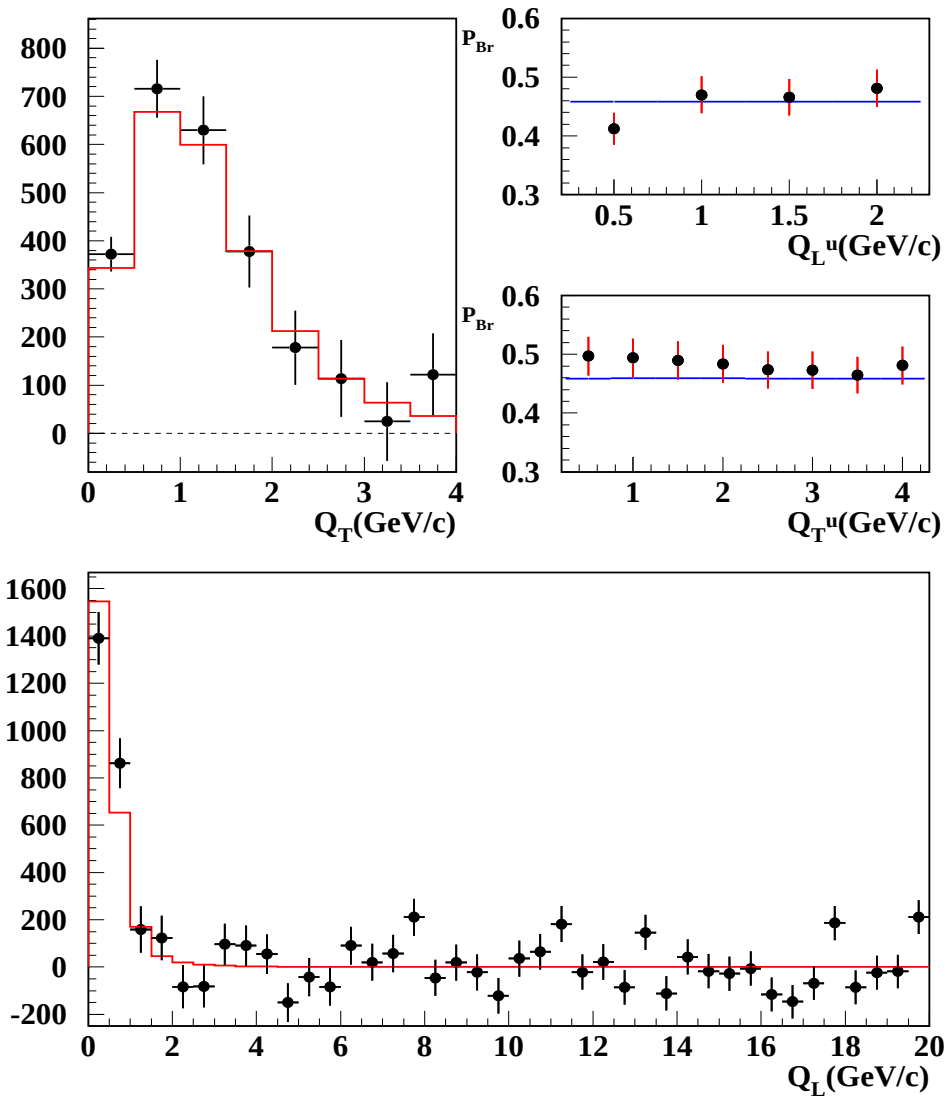

Fig. 13. *Fit results for the* $\pi^+\pi^-$ *momentum interval* $3.2 < p < 3.8$ *GeV/c in lab-frame. Caption is identical to figure 12 for the rest.*

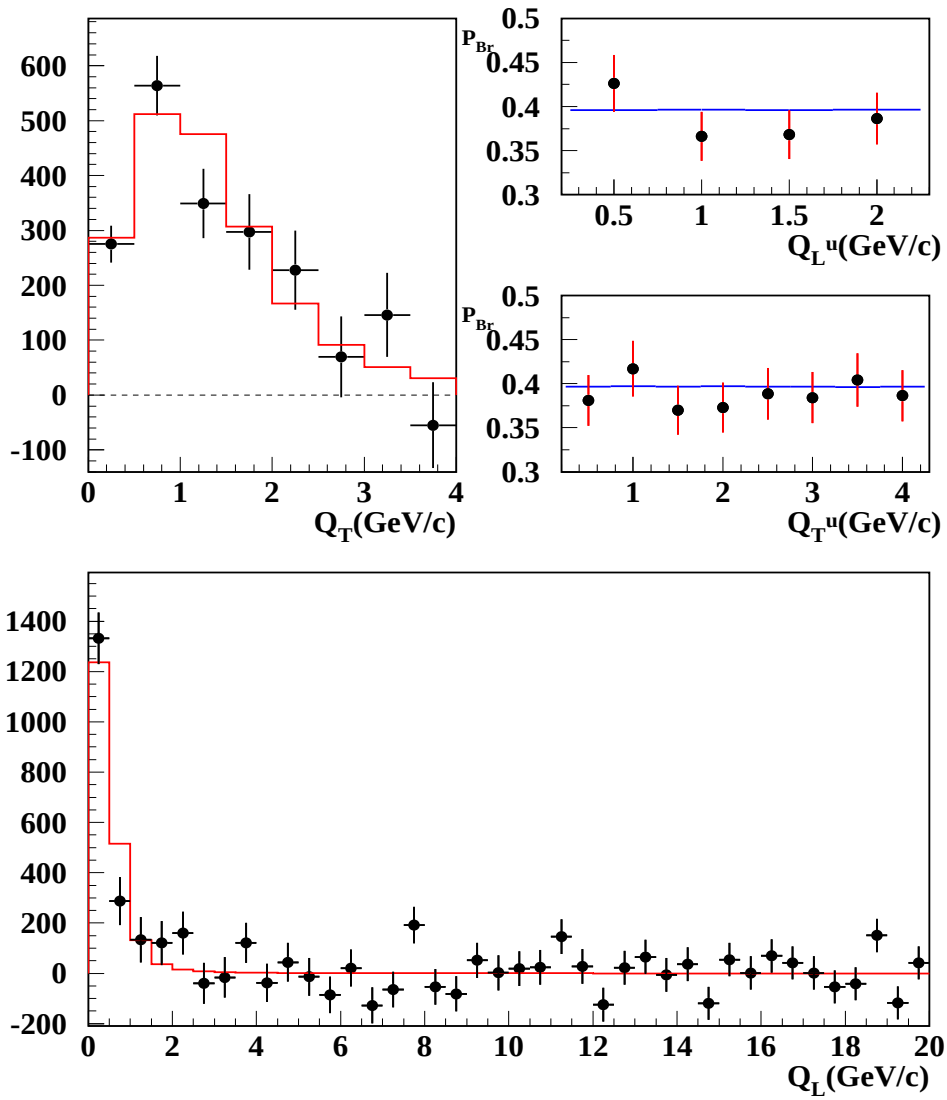

Fig. 14. *Fit results for the $\pi^+\pi^-$ momentum interval 3.8 $< p <$ 4.4 GeV/c in lab-frame. Caption is identical to figure 12 for the rest.*

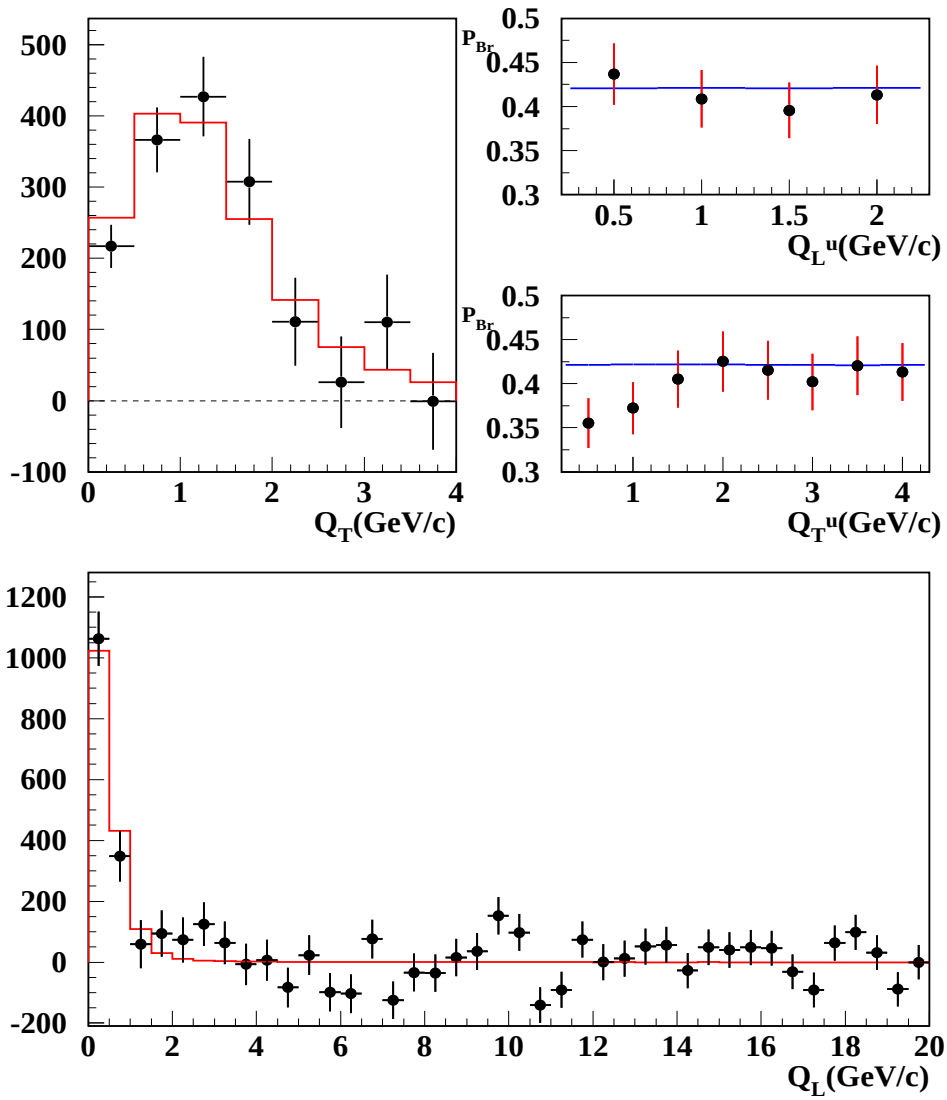

Fig. 15. *Fit results for the $\pi^+\pi^-$ momentum interval 4.4 $<$ p $<$ 5.0 GeV/c in lab-frame. Caption is identical to figure 12 for the rest.*

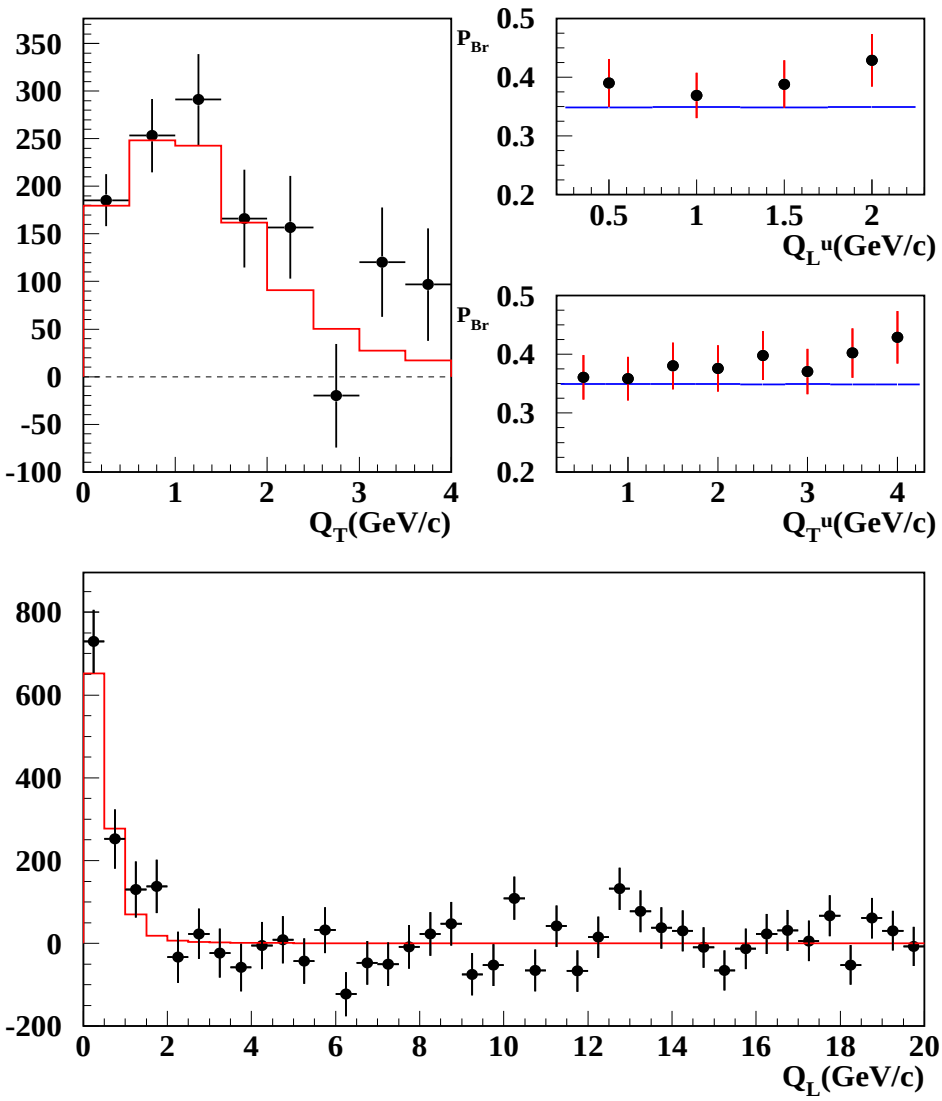

Fig. 16. *Fit results for the* $\pi^+\pi^-$ *momentum interval* $5. < p < 5.6$ *GeV/c in lab-frame. Caption is identical to figure 12 for the rest.*

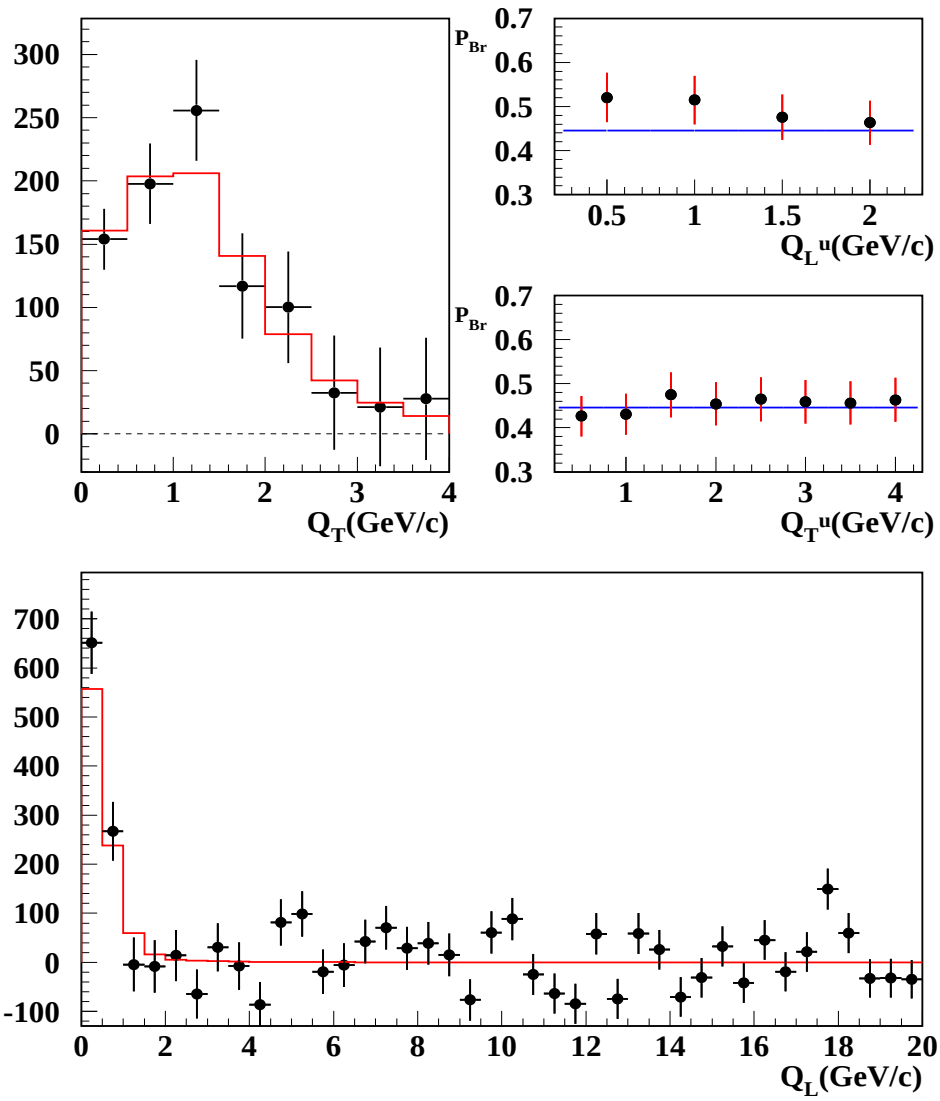

Fig. 17. *Fit results for the* $\pi^+\pi^-$ *momentum interval* $5.6 < p < 6.2$ *GeV/c in lab-frame. Caption is identical to figure 12 for the rest.*

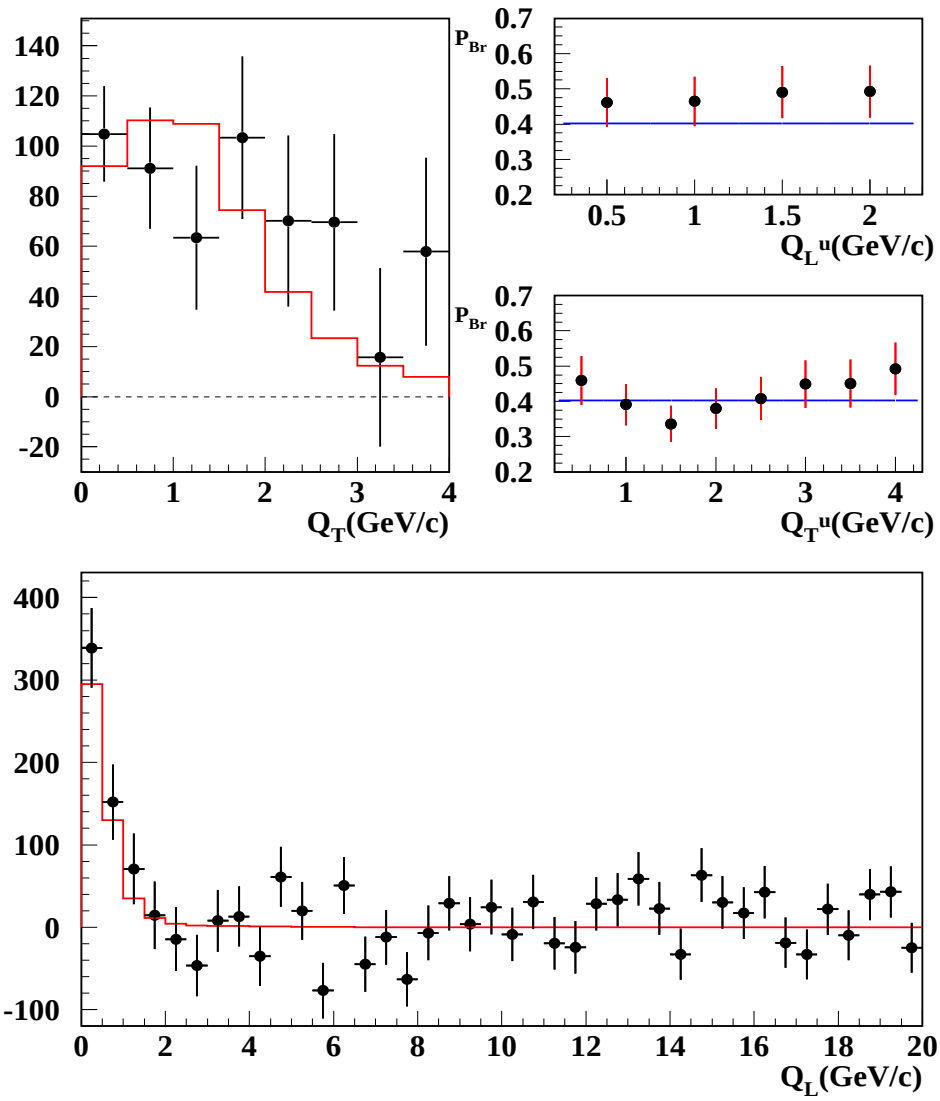

Fig. 18. *Fit results for the $\pi^+\pi^-$ momentum interval* $6.2 < p < 6.8$ *GeV/c in lab-frame. Caption is identical to figure 12 for the rest.*

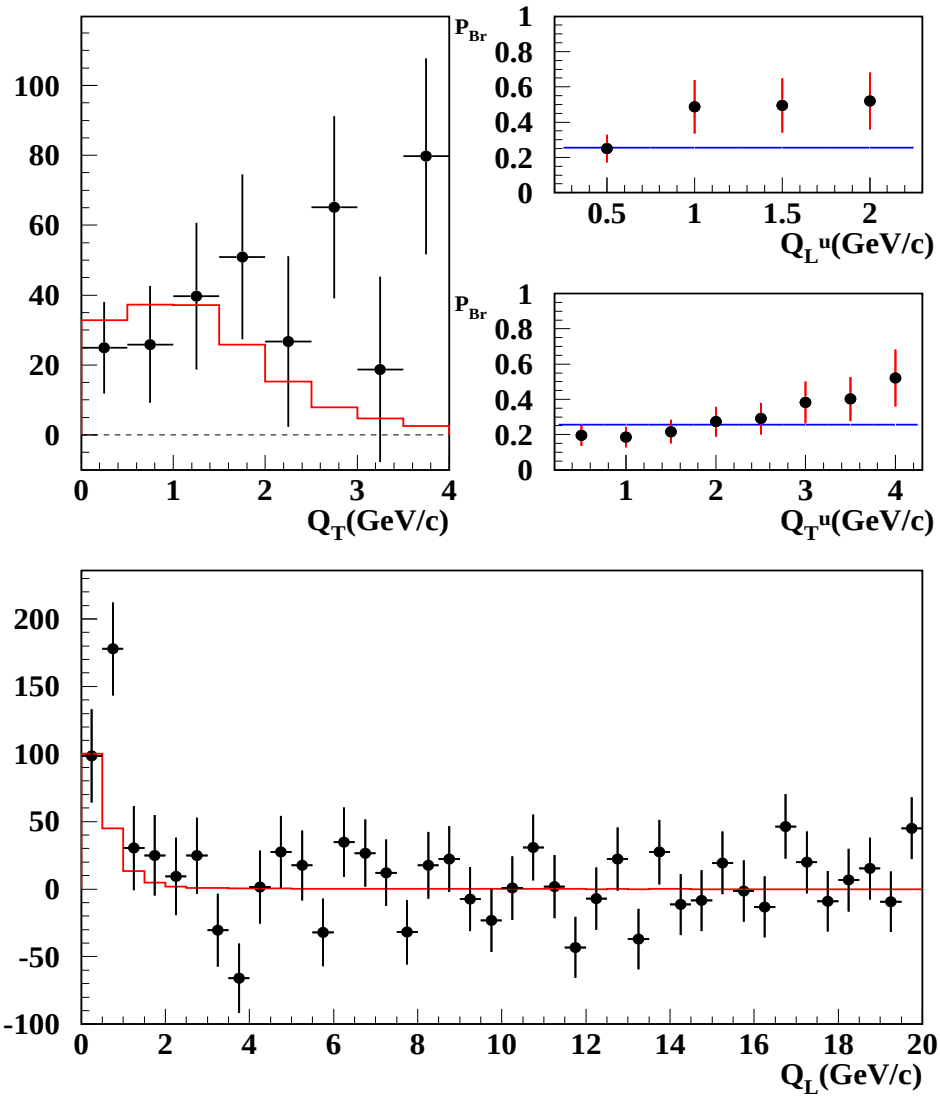

Fig. 19. *Fit results for the* $\pi^+\pi^-$ *momentum interval* $6.8 < p < 7.4$ *GeV/c in lab-frame. Caption is identical to figure 12 for the rest.*

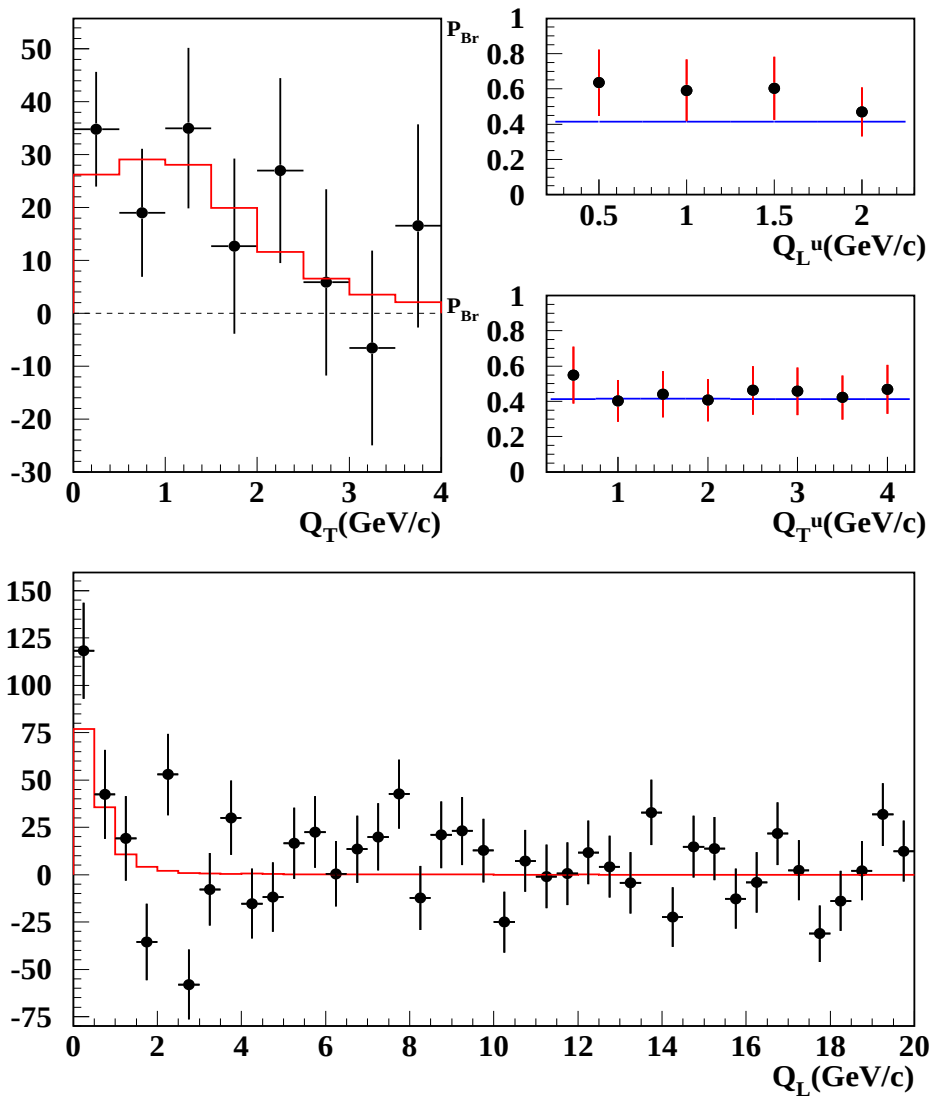

Fig. 20. *Fit results for the $\pi^+\pi^-$ momentum interval $7.4 < p < 8.0$ GeV/c in lab-frame. Caption is identical to figure 12 for the rest.*

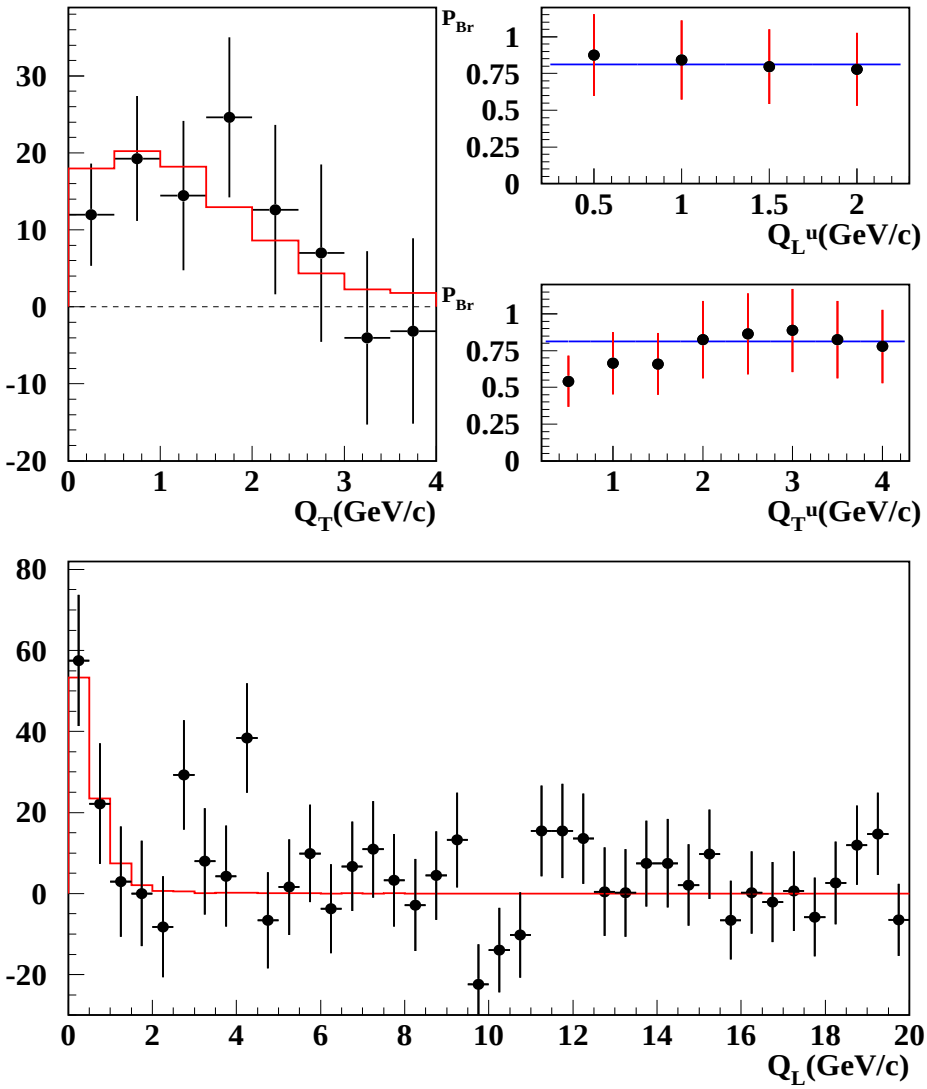

Fig. 21. *Fit results for the* $\pi^+\pi^-$ *momentum interval* $8.0 < p < 8.6$ *GeV/c in lab-frame. Caption is identical to figure 12 for the rest.*

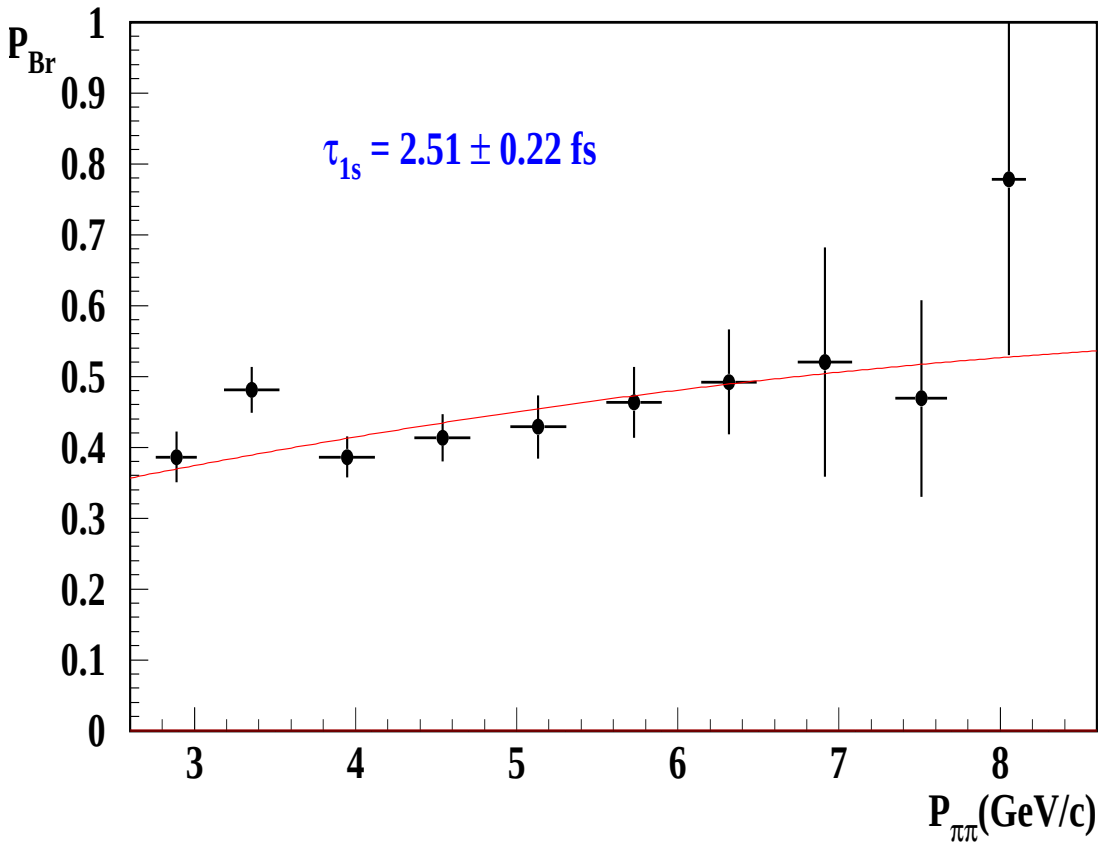

Fig. 22. *Pionium break-up probability P_{Br} as function of atom momentum, as compared to best fit Monte Carlo prediction with average Ni foil thickness. The fit χ^2 is 11.2 for 9 degrees of freedom. Pionium* 1*s lifetime value and error are indicated , for 2002+2003 data.*

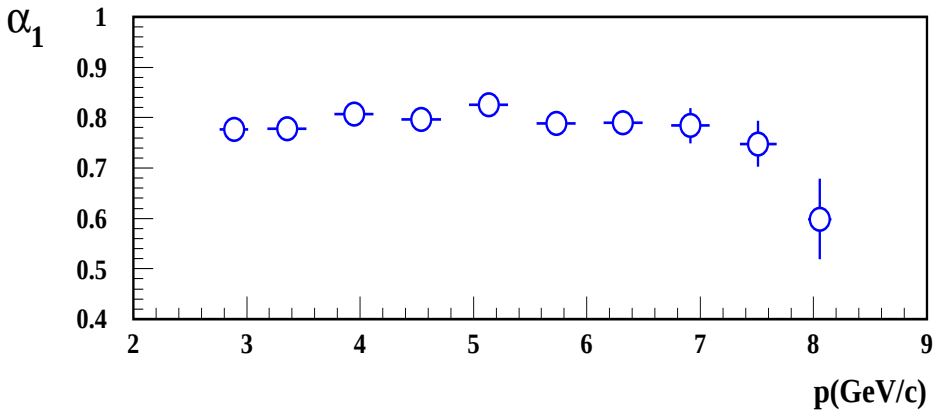

Fig. 23. *Fitted values of α_1 parameter as function of $\pi^+\pi^-$ momentum.*

The number of atom pairs N_A determined as function of p is plotted in figure 24 along with the number of Coulomb pairs given by the fit in each bin. Errors in N_A are given by MINOS variation of γ parameter. It is seen that atom production follows rather closely the spectrum of semi-inclusive $\pi^+\pi^-$ differential cross-section, as expected from bound state production. Please note that both of these spectra are uncorrected for spectrometer acceptance.

Pionium break-up probabilities can now be determined by using the momentum-dependent K-factors calculated in table 3, and they are shown in figure 22. Errors were propagated from those provided by the fit for N_A and N_C. P_{Br} values are compatible with a smooth increase with increasing atom momentum, as predicted by Monte Carlo tracking inside the target foil [7] [8]. We generate a continuous set of $P_{Br}(p)$ curves with varying values of the $1s$ Pionium lifetime (τ_{1s}). χ^2 minimization with respect to this set provides a measurement of τ_{1s} with an error.

The fitted values of α_1 parameter (fraction of Coulomb pairs) are also shown in figure 23 as function of p. They show a smooth behaviour.

In figure 25 we plot the number of non-Coulomb pairs determined by the fit as function of p, after subtraction of accidentals (see [2]), and we compare the spectrum with that previously determined for Coulomb pairs (see figure 24). The non-Coulomb spectrum is significantly softer than the Coulomb spectrum, probably due to parent multibody decays of the acompanying long-lifetime particle.

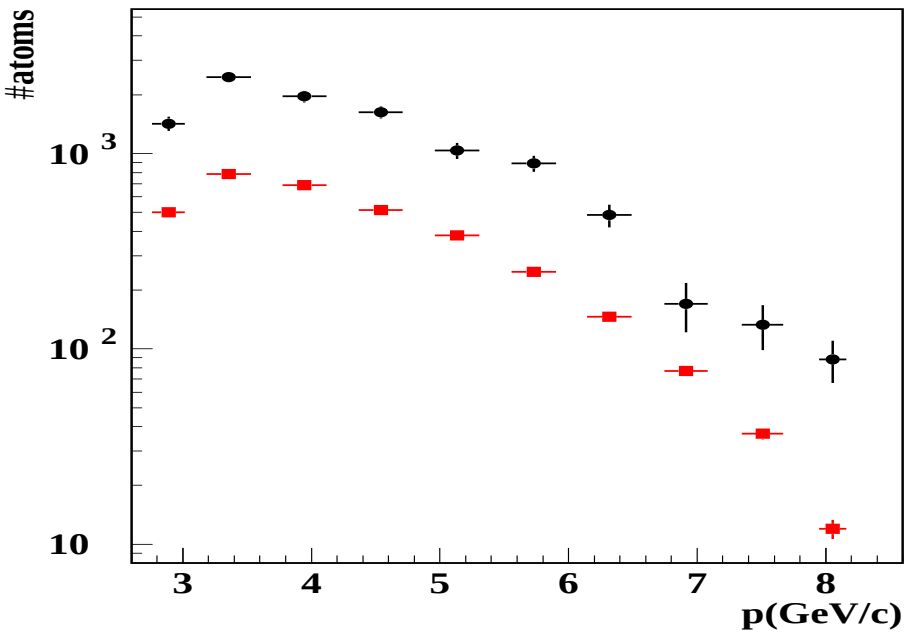

Fig. 24. *Fitted number of atom pairs as function of their lab-frame momentum (black circles) , as compared to the fitted number of Coulomb pais for $Q_L > 2MeV/c$ (coloured rectangles). The latter were normalized to half the area, to avoid the very large difference in actual scale.*

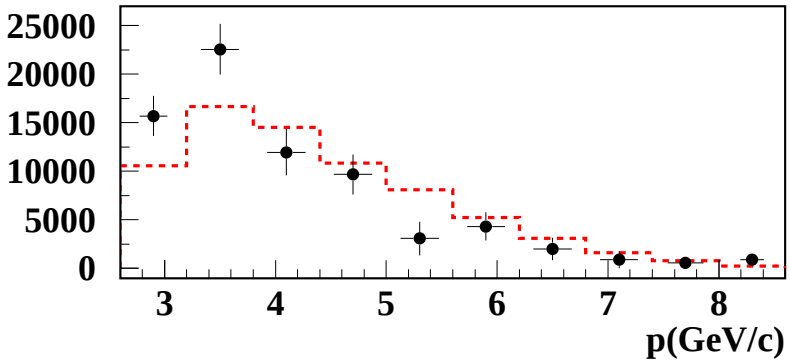

Fig. 25. *Fitted number of long-lifetime pairs (circles), determined from α_3 parameter, as function of $\pi^+\pi^-$ momentum. It is compared with the number of Coulomb pairs in figure 24 (dotted line), normalized to the same area.*

4 Systematic error

The discussion and conclusions concerning systematic errors reported in our previous publication (see section 5 and summary table 12 of note [1]), remains valid with the new 2002 and 2003 data. At least we can say there is no reason to think that any of the estimated error contributions are now larger. On the contrary, there are some indications that the new data might be subject to smaller systematic errors, such as:

- the improved quality of the Q_T spectrum, as a consequence of two newly constructed MSGC/GEM detector planes, and one extra SFD U-plane
- larger statistics of accidental pairs, to better describe the Q_L acceptance

Nevertheless, and lacking new specific studies, we stick to the overall systematic error estimation $\Delta P_{Br} = \pm 0.006$ for the breakup probability measurement with 2002+2003 Ni data.

5 Lifetime measurement

Pionium break-up probability P_{Br} in the Ni foil has been determined in two different ways. One is making a global (momentum-integrated) fit, which provides a single measurement for the average P_{Br}, and another is making 10 independent experiments to measure this quantity in $600 MeV/c$ wide intervals of Pionium momentum. The results are in very good agreement with each other when the average P_{Br} values are compared, and have equal statistical errors. Both of them provide a high fit quality with respect to the Monte Carlo hypothesis, in terms of χ^2 probability.

Taking into account the systematic error estimated in section 5, we have the break-up probability measurement:

$$P_{Br} = 0.427 \pm 0.013\ (stat) \pm 0.006\ (syst)$$

or having both error sources in quadrature:

$$P_{Br} = 0.427 \pm 0.015$$

Using the relationship between P_{Br} and lifetime obtained from the Pionium propagation code [7] [8], we determine the Pionium $1s$ lifetime from 2002+2003 data alone:

$$\tau_{1S} = 2.51\ ^{+0.24}_{-0.22}\ fs$$

6 Acknowledgements

We thank Cibrán Santamarina for help in utilization of his propagation code, and also Valeria Yazkov, Mikhail Zhabitsky and Juan J. Saborido for their indications.

This publication would not have been possible without the strong support of Centro de Supercomputación de Galicia (CESGA), which we would like to thank very specially. In particular Carlos Fernández Sánchez, in charge of the SVGD cluster at CESGA.

The construction of this experiment was funded in part by the spanish National Program for Particle Physics from Ministerio de Educación y Ciencia (MEC), under projects FPA2005-06441, AEN99-0488 and AEN96-1671, and also by the Xunta de Galicia under projects PGIDIT06PXIB206100PR and PGIDT00PXI20602PR. We also acknowledge the support received from Xunta the Galicia as "grupo de referencia competitiva" reference 2007/000062-0.

References

[1] DIRAC Note 07-07: Final Results for Pionium Lifetime Measurement with 2001 Data, A. Romero, B. Adeva, J. L. Fungueiriño, O.Vázquez Doce.

[2] DIRAC Note 06-03: Measurement of pionium lifetime, B.Adeva, A.Romero, O.Vazquez Doce.

[3] DIRAC note 06-05 : Experimental Measurement of a K^+K^- Signal at $p = 2.9GeV/c$ in Ni 2001 Data, B. Adeva, A. Romero and O. Vázquez Doce.

[4] DIRAC note 07-02 : Study of $K^{\pm}\pi^{\mp}$, K^+K^- and K^-p production in DIRAC using time-of-flight measurements , B. Adeva, A. Romero and O. Vázquez Doce, C. Mariñas, J. L. Fungueiriño. M. Bleicher et al., J. Phys. G25 (1999) 1859; hep-ph/9909407.

[5] DIRAC report "DIRAC targets", by A. Kuptsov, 5 March 2005.

[6] DIRAC Note 05-15: Full-Tracking Resolution in DIRAC with 2001 Data, B. Adeva, A. Romero and O. Vázquez Doce.
DIRAC Note 05-19: Addendum to Full-Tracking Resolution in DIRAC with 2001 Data, B. Adeva, A. Romero and O. Vázquez Doce.

[7] DIRAC note 04-02: DIRAC events generator, C. Santamarina.

[8] C. Santamaria, M. Schuman, L.G. Afanasyev, T. Heim, A Monte-Carlo Calculation of the Pionium Breakup Probability with Different Sets of Pionium Target Cross Sections, J. Phys. B. At. Mol. Opt. Phys. 36 4273 (2003), arXiv:physics/0306161 v1.